Physiol Genomics 15: 52–64, 2003;
10.1152/physiolgenomics.00139.2002.

The graft response to transplantation: a gene expression profile analysis

Kenneth Christopher,[1] Thomas F. Mueller,[1] Rachel DeFina,[1] Yurong Liang,[1] Jianhua Zhang,[2] Robert Gentleman,[2] and David L. Perkins[1]

[1]*Laboratory of Molecular Immunology, Department of Medicine, Brigham and Women's Hospital, Harvard Medical School; and* [2]*Biostatistics Unit, Department of Biostatistical Science, Dana-Farber Cancer Institute, Harvard Medical School, Boston, Massachusetts 02115*

Submitted 17 October 2002; accepted in final form 18 July 2003

Christopher, Kenneth, Thomas F. Mueller, Rachel DeFina, Yurong Liang, Jianhua Zhang, Robert Gentleman, and David L. Perkins. The graft response to transplantation: a gene expression profile analysis. *Physiol Genomics* 15: 52–64, 2003; 10.1152/physiolgenomics.00139.2002.—Little is known regarding the graft response to transplantation injury. This study investigates the posttransplantation response of genes that are constitutively expressed in the heart. Constitutive heart and lymph node tissue-restricted gene expression was first analyzed with DNA microarrays. To demonstrate changes following transplantation in genes constitutively expressed in the heart, we performed vascularized murine heart transplants in allogeneic (BALB/c to B6), syngeneic (B6 to B6), and alymphoid (BALB/c-RAG2$^{-/-}$ to B6-RAG1$^{-/-}$) experimental groups. Temporal induction of genes posttransplant relative to constitutive expression was evaluated with DNA microarrays. Dendrograms and self-organizing maps were generated to determine the dissimilarity between the experimental groups and to identify subsets of differentially expressed genes within the groups, respectively. Expression patterns of selected genes were confirmed by real-time PCR. Biological processes were assigned to genes induced posttransplant using the AnnBuilder package via the Gene Ontology Database. Posttransplant, a shift was noted in genes classified as defense, communication, and metabolism. Our results identify novel components of the graft response to transplantation injury and rejection.

gene regulation; rodent

THE PROCESS OF ALLOGRAFT REJECTION involves a robust inflammatory and immune response that is mediated by effector cells infiltrating the graft. In previous studies, we have focused on the innate immune response to the graft posttransplantation (4, 11). A poorly understood corollary is the graft response to transplantation. Little is known regarding the graft response to the surgical wounding, stress, ischemia, and rejection associated with transplantation. Thus the objective of this study was to evaluate the graft response to transplantation injury.

Our assumption was that the graft response would be complex, involve multiple genes, and be detectable as changes in gene expression. A previous report analyzing global expression profiles of both mRNA and protein found that 94% of differentially regulated genes had detectable changes in the level of mRNA (13). This suggests that a substantial proportion of differential regulation involves detectable changes in transcription or mRNA stability. Our experimental design thus uses DNA microarrays to monitor the expression of large subsets of genes that demonstrate differential constitutive tissue-restricted expression. Based on the presence or absence of constitutive gene expression in untransplanted heart (graft source) or lymph node (phenotype of at least a portion of the infiltrating cells), we assigned genes to one of four of the following subsets: *1*) heart restrictive, *2*) lymph node restrictive, *3*) expressed in neither heart nor lymph node (neither subset), and *4*) expressed in both heart and lymph node (both subset). To differentiate changes in gene expression due to adaptive immunity vs. antigen-independent mechanisms, expression of each tissue-restricted subset gene was compared with our microarray database (4) generated to evaluate gene expression in alymphoid, syngeneic, and allogeneic experimental groups of heart transplantation. The alymphoid group consists of recombinase activating gene (RAG)-deficient donors and recipients that lack functional T and B cell antigen receptors and thus cannot mount an adaptive immune response. The syngeneic group eliminates the presence of alloantigen by using genetically identical donor and recipient strains. The allogeneic group uses donor and recipient strains with a complete major histocompatibility complex (MHC) class I and II mismatch. This experimental approach should suggest gene subsets expressed by the graft tissue that are differentially regulated following transplantation.

To identify small numbers of groups of genes based on similar expression patterns we turned to the self-organizing map (SOM) algorithm. The SOM algorithm is an artificial neural network that has been used in many different engineering and scientific applications such as image recognition, signal processing, and gene expression analysis (23). Because of its high classification power, the SOM is an efficient strategy for mining

Article published online before print. See web site for date of publication (http://physiolgenomics.physiology.org).

Address for reprint requests and other correspondence: D. L. Perkins, Laboratory of Molecular Immunology, Brigham and Women's Hospital, PBB 170 75 Francis St., Boston, MA 02115 (E-mail: dperkins@rics.bwh.harvard.edu).

a wide range of genomic information from large numbers of sequences. Using a combination of hierarchical clustering algorithms and SOMs, we identified unique profiles of gene expression in each experimental group. These profiles identified modulated gene expression in both the cardiac-restricted and lymph node-restricted categories. To illustrate changes of biological functions between and within the experimental groups, each gene identified in the profiles was assigned a broad biological process via the Gene Ontology database (1). Gene Ontology is designed to produce a controlled vocabulary that applies to all eukaryotes. Biological processes are defined as broad biological goals (i.e., defense). The assignment of individual genes to biological processes allows for a broad perspective on differential gene expression.

Current immunosuppressive treatments commonly used in clinical transplantation are directed at the adaptive immune response, in particular, the T cell response. Our findings show that transplantation elicits a differential genomic profile within the graft of increasing expression of genes involved in the biological processes of defense and cell communication. Genes constitutively expressed in the graft prior to transplantation which are upregulated at *day 1* following transplantation are those involved in cytoprotection. Genes upregulated at *day 7* following transplantation include genes involved in innate immunity and cytoprotection. Our results provide novel insights and identify components of the graft response to the complex process of transplantation.

METHODS

Mice. Eight to 12-wk-old male mice including BALB/cByJ (BALB/c) (H-2^d), C57BL/6J (B6) (H-2^b), C57BL/6J-Rag-1^{tm1Mom} (B6-Rag) (H-2^b) (Jackson Laboratories, Bar Harbor, MA), and BALB/c-AnNTac-Rag2^{tm1}N12 (BALB/c-Rag) (H-2^d) (Taconic) were used as donor and recipients in the transplant experiments. H-2 refers to the murine major histocompatibility complex. An MHC haplotype (H-2^b, H-2^d) is the haploid chromosomal combination of alleles of MHC loci in a given mouse strain. Mice are maintained in vented racks with constant temperature and humidity in our animal facility under virus-antibody-free conditions.

Vascularized heterotopic cardiac transplantation. Murine hearts were transplanted as previously described (5). Briefly, hearts were harvested from freshly killed donors and immediately transplanted into 8- to 12-wk-old recipients that were anesthetized intraperitoneally with 60 μg/kg of pentobarbital sodium. The donor aorta was attached to the recipient abdominal aorta by end-to-side anastamosis, and the donor pulmonary artery was attached to the recipient vena cava by end-to-side anastamosis. All surgical procedures were completed in less than 60 min from the time that the donor heart was harvested. Donor hearts that did not beat immediately after reperfusion or stopped within 1 day following transplantation were excluded (>95% of all grafts functioned at 1 day following transplantation). The native heart of the recipient was not surgically manipulated and remained functional. Donor grafts were harvested at 24 h or 7 days following transplantation and prepared for microarray analysis or real-time PCR.

DNA microarrays. Experimental procedures for the GeneChips were performed according to the Affymetrix GeneChip Expression Analysis Technical Manual. Briefly, double-stranded cDNA was synthesized by means of the SuperScript Choice system (Invitrogen, Carlsbad, CA) and a $T7(dT)_{24}$ primer (Genset Oligos, La Jolla, CA). The cDNA was purified using phenol/chloroform extraction with Phase Lock Gel (Eppendorf) and concentrated by ethanol precipitation. In vitro transcription was performed to produce biotin-labeled cRNA using a BioArray HighYield RNA Transcript Labeling Kit (Enzo Diagnostics, Farmingdale, NY) according to the manufacturer's instructions. cRNA was linearly amplified ~40-fold with T7 polymerase using double-stranded cDNA that was synthesized. The biotinylated RNA was cleaned with an RNeasy Mini kit (Qiagen, Valencia, CA), fragmented to 50 to 200 nt, and then hybridized to an Affymetrix murine array (Mu11kB), which contains probe sets for 6,500 genes and expressed sequence tags (ESTs). After being washed, the array was stained with streptavidin-phycoerythrin (Molecular Probes, Eugene, OR), amplified by biotinylated anti-streptavidin (Vector Laboratories, Burlingame, CA), and then scanned on an HP GeneArray scanner. The intensity for each feature of the array was captured with Affymetrix GeneChip Software, according to standard Affymetrix procedures.

Statistics and data analysis. Array data was analyzed with Microarray Suite 4.0. A single expression level for each gene was derived from the 20 probe pairs representing each gene, 20 perfectly matched (PM) and mismatched (MM) control probes. The MM probes act as specificity control that allow the direct subtraction of background and cross-hybridization signals. Each array was normalized to a standard of 2,500 units per probe set. To determine the quantitative RNA level, the average of the differences (avg diff) representing PM − MM for each gene-specific probe set was calculated. The expression of each probe set was categorized as present (P), marginal (M), or absent (A). Calculations of means and variances were performed with JMP statistical software (SAS Institute, Cary, NC).

Cluster analysis. Cluster analysis was performed using Cluster and TreeView (8) and GeneCluster software (23) software. Average difference values were analyzed by Cluster without normalization using the hierarchical clustering algorithm with average linkage clustering. Briefly, dissimilarity is determined by calculation of the Pearson correlation coefficient between each series of values from each experimental group (8). After processing, the dendrogram was visualized by TreeView. SOMs were generated by GeneCluster on genes showing a minimum of a twofold change among the experimental groups using a 2×3 geometry of six seed maps (23). Six maps were selected empirically to eliminate clusters with few genes or large standard deviations. The centroids and standard deviations of the groupings were analyzed using 100 epochs. Based on multiple heuristic observations, increased numbers of nodes produced clusters with low numbers of genes, whereas decreased numbers of nodes produced larger standard deviation. Increasing the number of epochs (=500) did not produce detectable changes in the clusters or standard deviations. SOM output is then graphically presented as a set of maps (Fig. 3 and 6) showing a relatively small group of genes that exhibit similar expression characteristics across all control and experimental conditions. Tables 2 and 3 list groups of genes with similar expression patterns as determined by the SOM algorithm output.

Gene Ontology Process assignment. The mapping of the GenBank accession numbers associated with a microarray

oligo sequence to Gene Ontology (GO) terms is performed using the AnnBuilder package of the Bioconductor project (**http://www.bioconductor.org**). The AnnBuilder package is an R-based system (**http://www.r-project.org**) that maps a given set of GenBank accession numbers to LocusLink identifiers and then to any data in a public database that can be linked to LocusLink identifiers. As both UniGene (Mm.data.gz) and LocusLink (LL_tmpl.gz) provide mappings between GenBank accession numbers and LocusLink identifiers with intersections, the GenBank accession numbers were first mapped to LocusLink identifiers using both sources. A unified mapping was obtained by including the mappings that were agreed by both sources, and the mapping by UniGene was included when they disagree. In a trial based on the genes on Affymetrix U95AV2 GeneChip, we only found 27 disagreements for a total of 12,625 genes.

The unified mapping was then used to process the LL_tmpl file from LocusLink to link GenBank accession numbers to GO identifiers and then to GO terms from the Gene Ontology Consortium (go.xml) using GO identifiers as the linkage for data. The end product of the mapping is an extended markup language (XML) file containing entries of GenBank accession numbers and the GO terms associated with each accession number. The tree structure of the GO terms was reflected by associating a GO term to the GenBank accession numbers mapped to the term as well as all the accession numbers mapped to the offspring of that GO term. The one-to-many relationship between GenBank accession numbers and GO terms was also maintained by associating all GO terms to all the related GenBank accession numbers. When a mapping was provided by only one source, that mapping was included in the unified mapping.

Based on the XML file generated by the AnnBuilder package, we then assigned biological processes as defined by the Gene Ontology database to the microarray data. The biological process is defined as the biological objective to which the gene contributes. Most of the genes analyzed could be assigned to the following five broad processes: cell communication, cell growth/ maintenance (including cell organization and biogenesis), metabolism, defense response, and the stress response. The AnnBuilder package cannot assign a biological processes to genes that do not have a GO identifier. Thus genes that do not have GO identifiers are not included in the Figs. 4 and 7. In Tables 2 and 3, genes without GO identifiers were assigned broad biological processes based on the function reported in the literature. A detailed description of each gene including the identifier, standard name, characterization, and relevant references, as well as related biological processes according to the GO classification is provided on our web site (**http://perkinslab.bwh.harvard.edu**).

Real-time quantitative PCR. Total murine heart RNA was individually isolated from three untransplanted control hearts, three *day 1* allogeneic graft hearts, and three *day 7* allogeneic graft hearts. Ten micrograms of RNA was separately reverse transcribed using SuperScript II RNase Reverse Transcriptase (GIBCO, Carlsbad, CA). Specific apolipoprotein E, C1qb subunit, calpactin I, collagen-α1, creatine kinase, cytochrome C oxidase ViaH, decorin, GAPDH, lactate dehydrogenase 2B, metallothionein-1, myosin light chain 2, smooth muscle γ-actin, troponin-I, and ventricular alkali myosin light chain primer pairs were designed using the Primer Express software (Applied Biosystems, Foster City, CA). Primer sequences used follow: apolipoprotein E, forward 5′-GAGCCGGAGGTGACAGATCA-3′, reverse 5′-CTCCCAGGGTTGGTTGCTT-3′; C1qb subunit, forward 5′-AGGACCATCAACAGCCCCTT-3′, reverse 5′-CTTTTCGAAGCGAATGACCTG-3′; calpactin I, forward 5′-CCAAGTGCCTACGGGTCAGT-3′, reverse 5′-CCTCTCAGCATCGAAGTTGGT-3′; collagen-α1, forward 5′-TGAAGATGTCGTTGATGTGCAG-3′, reverse 5′-CGGCTGGAAAGAAGTCTGAGG-3′; creatine kinase, forward 5′-AAGGTGCTGACCCCTGACCT-3′, reverse 5′-TGGTGTCTCCTTATCGCGAAG-3′; cytochrome C oxidase ViaH, forward 5′-TGACCTTTGTGCTGGCTCTTC-3′, reverse 5′-AGCAGTTAAGGGAGCAGAGGG-3′; decorin, forward 5′-AGCTTCAACAGCATCACCGTT-3′, reverse 5′-AGGAACATTGGCCAGACTGC-3′; GAPDH, forward 5′-TTGTGGAAGGGCTCATGACC-3′, reverse 5′-TCTTCTGGGTGGCAGTGATG-3′; lactate dehydrogenase 2B, forward 5′-CTGTAGTGGGCGTTGGACAA-3′, reverse 5′-CCAGAATGCTGATGGCACAT-3′; metallothionein-1, forward 5′-TGCTCCACCGGCGG-3′, reverse 5′-TTTGCAGACACAGCCCTGG-3′; myosin light chain 2, forward 5′-CACTTCTCCTTGGTCCACTATGC-3′, reverse 5′-GCCCATAATGTTGTAGTCCACG-3′; smooth muscle γ-actin Actg2, forward 5′-TGTGTGACAATGGCTCTGGC-3′, reverse 5′-CATCATCTCCTGCAAAGCCTG-3′; troponin-I, forward 5′-CCCACCTCAAGCAGGTGAA-3′, reverse 5′-CCTCCCGGTTTTCCTTCTCA-3′; and ventricular alkali myosin light chain, forward 5′-AGAGAAACTGATGGCTGGTCAAG-3′, reverse 5′-TCATAGTTGATGCAGCCGTTG-3′. Direct detection of the PCR product is monitored by measuring an increase in fluorescence due to the binding of SYBR Green to double-stranded DNA. Reactions are performed in a MicroAmp Optical 96-well reaction plate (Applied Biosystems) using for each separate well 5 μl of cDNA mix, 5 μl of primer, and 10 μl of SYBR Green Master Mix (Applied Biosystems). Each well contains the primer pair for amplification of one of the parameters of interest. The gene-specific PCR products are continuously measured by means of the GeneAmp 5700 Sequence Detection System (Applied Biosystems) during 40 cycles. The threshold cycles, i.e., the PCR cycle at which an increase in reporter fluorescence above a baseline signal can first be detected, of each target product is determined and set in relation to the amplification plot of housekeeping gene GAPDH. All experiments are run in duplicate, and the same thermal cycling parameters are used. Nontemplate controls and dissociation curves are used to detect primer-dimer conformation and nonspecific amplification. Fold change is calculated relative to control heart cycle threshold (C_T). The C_T value is defined as the number of PCR cycles required for the fluorescence signal to exceed the detection threshold value. With the PCR efficiency of 100%, the C_T values of two separate genes can be compared (ΔC_T), and the fold difference $= 2^{-(C_T - C_{Tcontrol})} = 2^{-\Delta C_T}$.

RESULTS

To determine baseline constitutive tissue-restricted gene expression, we analyzed RNA from two untransplanted control hearts and control lymph node with DNA microarrays. Results were analyzed with Microarray Suite software to calculate absolute difference values and to determine absent or present calls for each gene. This analysis indicated that in the untransplanted control tissues, 343 genes were expressed only in heart, 301 only in lymph node, 479 in both heart and lymph node (both subset), and 1,492 in neither heart nor lymph node (neither subset) (Fig. 1). Based on this analysis, those genes were then assigned to one of the four subsets (heart-restricted, lymph node-restricted, both, or neither). Changes in gene expression following transplantation of the four subsets were then determined by comparison to our murine array databank (one array per experimental condition)(4). Although

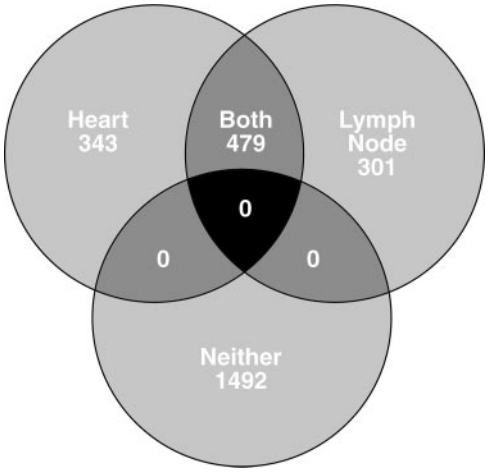

Fig. 1. Order-three Venn diagram of categories of constitutive gene expression. Categories include heart only (343 genes), lymph node only (301 genes), both heart and lymph node (479 genes), and neither heart nor lymph node (1,492 genes). Genes with upregulation of less than a twofold change in expression relative to mean expression were excluded.

the murine array (Mu11kB) contains probe sets for 6,500 genes and ESTs, only 5% of the probes are related to the immune response (Fig. 4*A*).

To analyze changes in gene expression following transplantation, we performed vascularized murine heart transplants in allogeneic (BALB/c > B6), syngeneic (B6 > B6), and alymphoid (BALB/c-RAG2$^{-/-}$ > B6-RAG1$^{-/-}$) experimental groups (Table 1). The alymphoid group, which lacks a functional adaptive immune response, used both donor and recipient mice deficient in the RAG gene, which is necessary to produce functional T and B cell antigen receptors. The donor and recipient mice in the syngeneic group were genetically identical. Thus both the alymphoid and syngeneic groups lack an alloantigen-driven adaptive immune response, and all changes in gene expression are attributed to antigen-independent mechanisms. In contrast, the allogeneic group has a complete MHC class I and II mismatch, plus minor antigen differences, and rejects grafts with a potent adaptive immune response in ~8 days.

We analyzed changes in the expression of genes in transplanted tissue according to one of the four subsets (heart-restricted, lymph node-restricted, both, or neither). We began by assessing changes of expression posttransplantation in the heart-restricted subset. To determine dissimilarity of genes expression between the experimental groups, we generated dendrograms with hierarchical clustering algorithms. The dissimilarity between groups in the dendrogram is calculated as the sum of the Pearson correlation coefficients between expression values of genes from each group. Figure 2*A* demonstrates the changes in gene expression at *day 1* following transplantation. As expected, lymph node is markedly dissimilar from the control and graft heart groups. The syngeneic and alymphoid groups show only mild dissimilarity and modestly differ from the allogeneic group. Although the Fig. 2*A* groups allogeneic *day 1* separate from syngenic and alymphoid *day 1*, the dissimilarity distances are quite small relative to that of the lymph node. Because of the small dissimilarity distances, a firm conclusion relative to the relationship of differential gene expression found in allogeneic, syngenic, and alymphoid *day 1* grafts is not possible. However, in the kinetic analysis at *day 7*, the allogeneic group is most similar to lymph node and markedly dissimilar from the control and *day 1* group (Fig. 2*B*). Thus the dendrograms in Fig. 2 serve to illustrate that the gene expression pattern in the allogeneic graft at *day 1* changes at *day 7* to an expression pattern more similar to that of a lymph node.

To identify subsets of genes within the heart-restricted subset that were differentially expressed in the experimental groups, we generated SOMs analyzing expression in control heart (BALB), control heart (B6), alymphoid graft heart *day 1*, allogeneic graft heart *day 1*, allogeneic graft heart *day 7*, and untransplanted control lymph node (Fig. 3 and Table 2). Table 2 lists the complete output of maps generated for the heart-restricted subset. In Fig. 3, *map 1* generated a list of genes upregulated in all groups (alymphoid and allogeneic *days 1* and *7*) following transplantation. Genes in *map 1* (Fig. 3) have previously reported associations with stress and injury responses and include αB2-crystallin, metallothionein-1, and collagen-α1. *Maps 2* and *3* (Fig. 3), which are similar, generated lists of genes (Table 2) that are downregulated follow-

Table 1. *Heterotopic cardiac transplant experimental groups*

Group	Donor	Donor H-2	Recipient	Recipient H-2
Alymphoid	BALB/c-RAG2$^{-/-}$	d	B6-RAG1$^{-/-}$	b
Syngeneic	B6	b	B6	b
Allogeneic	BALB/c	d	B6	b

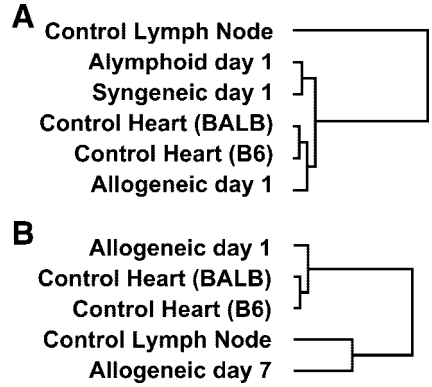

Fig. 2. Dendrogram of expression following transplantation of genes constitutively expressed in the heart. Agglomerative hierarchical clustering algorithm was used to generate dendrogram of experimental groups including allogeneic graft heart (*day 1*), alymphoid graft heart (*day 1*), syngeneic graft heart (*day 1*), untransplanted control heart (BALB), untransplanted control heart (B6), and control lymph node (*A*); and allogeneic graft heart (*day 1*), allogeneic graft heart (*day 7*), untransplanted control heart (BALB), untransplanted control heart (B6), and control lymph node (*B*). The *x*-axis distance is proportional to the dissimilarity between groups.

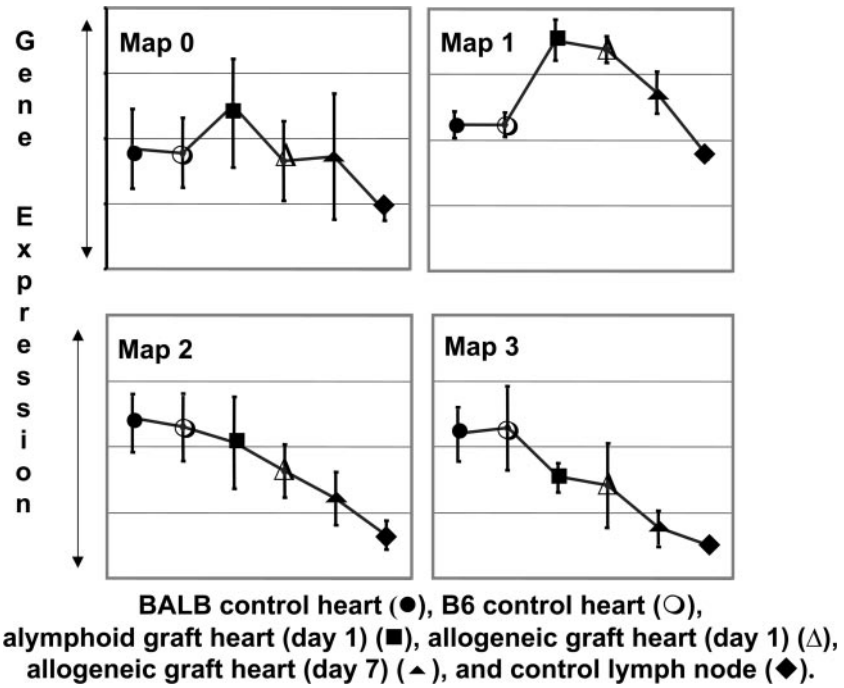

Fig. 3. Self-organizing map (SOM) of expression following transplantation of genes constitutively expressed in heart. Clusters of genes with similar patterns of expression in the experimental groups were identified using SOMs. Experimental groups distributed on *x*-axis include untransplanted BALB control heart (●), untransplanted B6 control heart (○), alymphoid graft heart (*day 1*) (■), allogeneic graft heart (*day 1*) (△), allogeneic graft heart (*day 7*) (▲), and control lymph node (◆). The *y*-axis is relative gene expression, which is auto-scaled to enhance visualization and thus variable among the maps. The mean expression is depicted as the symbols with error bars indicating 2 standard deviations. The number of genes in each cluster is 57 (*map 0*), 6 (*map 1*), 21 (*map 2*), and 9 (*map 3*). The algorithm was initiated with 2×2 geometry using 100 epochs. Genes corresponding to each map are listed in Table 2.

ing transplantation and include cytochrome c, troponin-I, and myoglobin. Interestingly, we did not detect a subset of constitutive heart genes highly upregulated in the allogeneic group at *day 7*. This observation suggests that the similarity observed between the control lymph node and allogeneic *day 7* groups in the dendrogram is due to the loss of constitutively expressed cardiac genes, rather than the gain of lymph node related genes in graft heart sample.

Biological process assignment following transplantation of the genes upregulated in the heart-restricted subset at *day 1* (Fig. 4*B*) shows cell maintenance (33%) and cell communication (42%) are prominent. At *day 7* (Fig. 4*C*), the stress and immunologic consequence of transplantation is reflected with increases in the expression of defense (22%) and metabolism genes (17%). The majority of heart-restricted subset genes downregulated at *day 1* following transplantation (Fig. 4*D*) assigned by Gene Ontology are cell maintenance (56%) and metabolism (27%). The proportion of heart-restricted subset genes downregulated genes at *day 7* (Fig. 4*E*) following transplantation was similar to *day 1*. This observation suggests the transcriptional program is altered in favor of defense genes at the expense of genes involved in cell growth and maintenance. Genes assigned to metabolism were both up- and downregulated in response to transplantation, which is illustrative of the complexity of the graft response to transplantation.

To assess changes of expression posttransplant in the "neither" genes subset, we generated hierarchical dendrograms. The neither subset should contain genes not constitutively expressed in heart or lymph node, but might be inducible following transplantation in either graft tissue or infiltrating cells. Analysis of changes in expression at *day 1* following transplantation of the neither subset showed only low levels of dissimilarity, even between the lymph node and heart tissues (Fig. 5*A*). This observation is consistent with the fact that the genes are not constitutively expressed but are upregulated to low levels of expression following transplantation. Similarly, the kinetic dendrogram shows only low levels of dissimilarity even in the *day 7* allogeneic and lymph node groups (Fig. 5*B*). Detection of specific subsets of genes with similar expression profiles using SOM identified small numbers of genes with these characteristics relative to the heart-restricted and lymph node-restricted categories (Fig. 6 and Table 3). *Map 0* (Fig. 6) contains genes that were upregulated in all groups following transplantation but not expressed constitutively. Consistent with this profile, genes included in this subset are IFN-β and 24p3. *Map 1* (Fig. 6) contains 11 genes upregulated at *day 1*, but not *day 7*, following transplantation and includes Eta-1/osteopontin, fibronectin, ngal, and gly96. Taken together, genes from the neither subset include a small number of genes induced following transplantation.

To identify the temporal induction of genes posttransplant we compared gene expression of allogeneic *day 1* and allogeneic *day 7* to control heart. The 343 heart-restricted subset genes (Fig. 1) were identified in the posttransplant allogeneic *day 1* and *day 7* microarray data. The expression values were normalized and expressed in standard deviation (z) units. The normalized values of each individual control B6 and BALB/c gene were averaged to obtain a control z value of that particular gene. The difference in gene expression between normalized control and allogeneic data sets was calculated (Tables 4 and 5). To limit changes based on background noise, normalized gene expression difference values Δz greater than 0.1 and less than -0.1

Table 2. *Heart-restricted subset self-organizing map output*

Map	ID	Abbreviation	Description	Gene Ontology Biological Process (secondary biological process)
Map 0	X13297	Acta2	vascular smooth muscle α-actin	cell organization/biogenesis (cytoskeleton organization and biogenesis)
	W58987	Actc1	md58d11.r1 EST	cell organization/biogenesis (cytoskeleton)
	D00466	Apo E	apolipoprotein E	cell growth and/or maintenance (lipid transport)
	X61600	β-enolase	β-enolase	metabolism (glycolysis)
	M22531	C1q B	C1q B chain	defense response (complement activation, classic pathway)
	ET62967	C1qC	C1q, c chain precursor	defense response (complement activation, classic pathway)
	X66295	C1qC	C1q C-chain	defense response (complement activation, classic pathway)
	D10024	Calpactin	calpactin I heavy chain	defense response (inflammatory response)
	L23108	CD36	CD36	cell communication (cell adhesion)
	W98255	CD81	me74g02.r1 EST	defense response (immune response)
	X58251	COL1A2	pro-α2(I) collagen	cell communication (cell adhesion)
	W18601	Cox5b	mb97a03.r1 EST	metabolism (electron transport)
	W91222	Cox7a3	mf85c05.r1 EST	metabolism (electron transport)
	Z38015	DMR-N9	myotonic dystrophy protein kinase	unknown
	W29562	Fabp4	mc03d09.r1 EST	metabolism
	J04953	Gelsolin	gelsolin	cell organization and biogenesis (actin filament organization)
	U13705	GPX3	glutathione peroxidase	metabolism (perioxidase reduction)
	D12907	Hsp47	47-kDa heat shock protein	cell communication (heat shock response)
	X51905	LDH2B	lactate dehydrogenase-B	metabolism (glycolysis)
	U07159	MCAD	medium-chain acyl-CoA dehydrogenase	metabolism (fatty acid metabolism)
	X06086	MEP	major excreted protein	metabolism
	D00613	Mglap	matrix Gla protein	developmental processes (ossification)
	X04972	MnSOD	manganese superoxide dismutase	stress response
	W13586	Myla	ma93a02.r1 EST	cell organization/biogenesis (cytoskeleton), developmental process (muscle development)
	Z49204	NADP TH	NADP transhydrogenase	metabolism
	X83933	RyR type 2	ryanodine receptor type 2	stress response
	W99870	Sec61 a	mg26b09.r1 EST	cell growth/maintenance
	Z22866	Skelemin	skelemin	cell growth and/or maintenance (striated muscle contraction), developmental processes (muscle development)
	X04017	SPARC	cysteine-rich glycoprotein	cell organization/biogenesis (cytoskeleton)
	X62940	TSC-22	TSC-22	metabolism (transcriptional regulation)
	U30840	VDAC	voltage-dependent anion channel 1	metabolism
Map 1	X52046	Col3A1	collagen α-1	cell communication (cell adhesion)
	M73741	Crystallin	αB2-crystallin	developmental processes (sensory organ development)
	V00835	MT-1	metallothionein-1	stress response
Map 2	W34687	ACTA1	mc33d02.r1 EST	cell growth and/or maintenance (striated muscle contraction)
	AA153484	Atp2a2	mr84h03.r1 EST	cell growth and/or maintenance (calcium ion transport)
	X52886	Cat D	cathepsin D	metabolism
	U08439	COX VIaH	cytochrome c oxidase ViaH	metabolism (electron transport)
	AA028501	COX8	mi19b12.r1 EST	metabolism (electron transport)
	X53929	Decorin	PGII decorin	metabolism (carbohydrate)
	X51905	LDH2B	lactate dehydrogenase 2B	metabolism (glycolysis)
	X01756	MC1	cytochrome c	metabolism (electron transport)
	X63349	TYRP	tyrosinase-related protein-2	cell growth/maintenance
Map 3	X03233	CK	muscle creatine kinase	metabolism
	W13236	M-CK	ma93a11.r1 EST	metabolism
	X67685	Mylc	ventricular alkali myosin light chain	cell organization/biogenesis (cytoskeleton organization and biogenesis) developmental processes (muscle development)
	M91602	MLC-2	myosin light chain 2	cell organization/biogenesis (cytoskeleton organization and biogenesis)
	M76601	Myhca	α-cardiac myosin heavy chain	cell organization/biogenesis (cytoskeleton), developmental process (muscle development), cell growth and/or maintenance striated muscle contraction) (protein modification)
	X04405	Myoglobin	myoglobin	metabolism
	W64587	SERCA2	md89g12.r1 EST	cell growth and/or maintenance (calcium ion transport)
	Z22784	Tn I	troponin-I	cell growth and/or maintenance (striated muscle contraction) (muscle contraction regulation)

Genes identified in each map output are listed in alphabetical order.

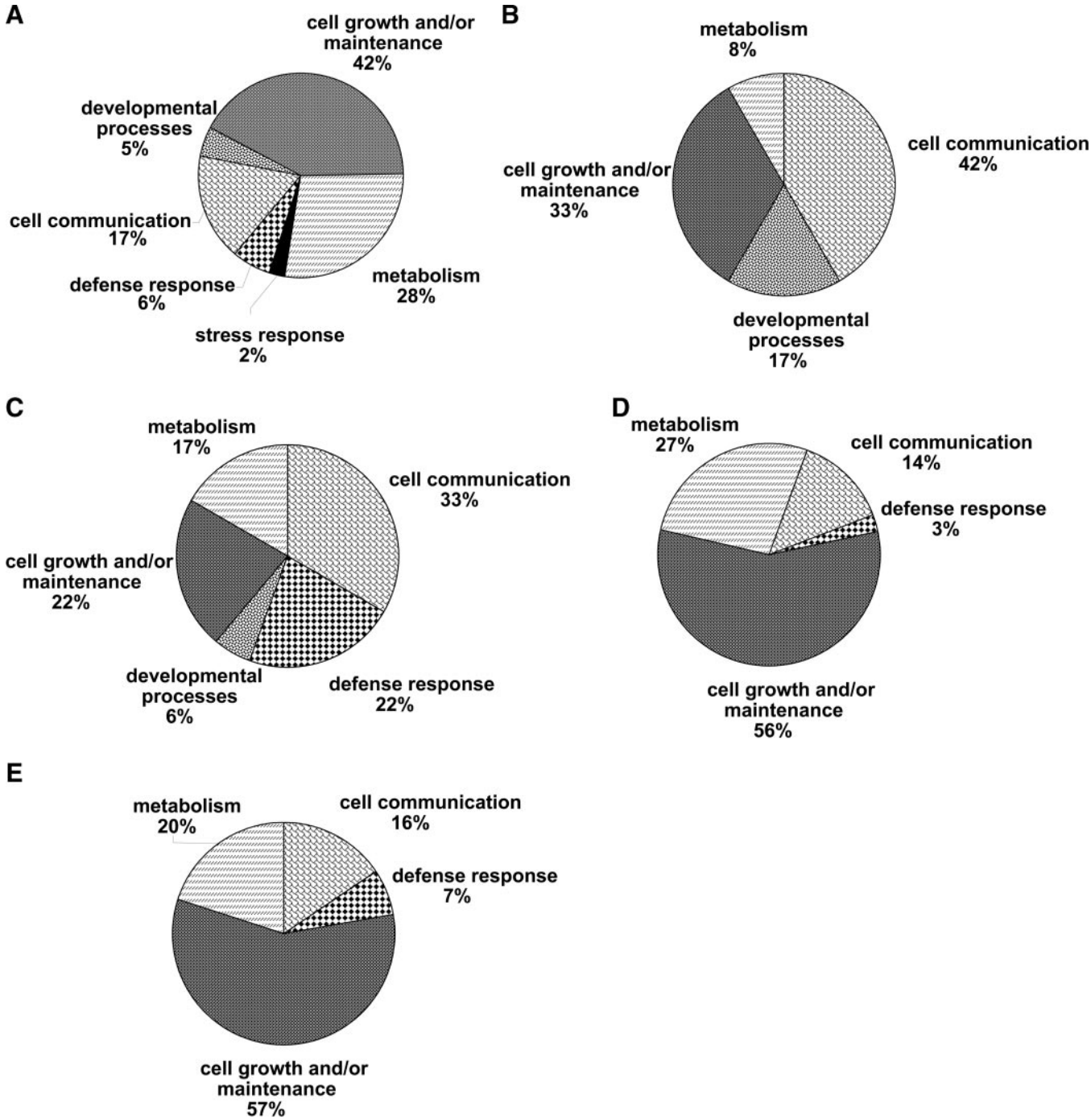

Fig. 4. AnnBuilder package output of the Gene Ontology defined biological processes based on the entire mu11kB GeneChip (*A*) and genes constitutively expressed in heart upregulated posttransplantation at *day 1* (*B*) or *day 7* (*C*). Pie charts of biological processes based on genes constitutively expressed in heart subsequently downregulated at *day 1* (*D*) or *day 7* (*E*) posttransplantation. Up- or downregulation is determined by normalized gene expression values at *day 1* or *day 7* less normalized heart control values.

were considered minimal for differential gene expression from control tissue. Heart-restricted subset genes with the largest increase in normalized expression values ($\Delta z > 1.2$) in the allogeneic *day 1* relative to control include αB2-crystallin, metallothionein-1, and collagen-α1 (Table 4). Heart-restricted subset genes with the largest increase in normalized expression values ($\Delta z > 2.5$) in the allogeneic *day 7* relative to control include C1qc, apolipoprotein E, C1qa, and C1qb (Table 5). This observation is consistent with the presumption that between *days 1* and *7*, differential expression of graft genes likely reflects the response of the graft to the graft ischemia and or surgical stress of transplantation at *day 1* followed by an antigen-inde-

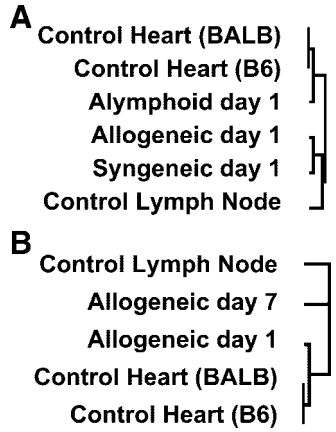

Fig. 5. Dendrogram of posttransplantation expression of genes constitutively expressed in neither heart nor lymph node. Agglomerative hierarchical clustering algorithm was used to generate dendrogram of experimental groups including allogeneic graft heart (*day 1*), alymphoid graft heart (*day 1*), syngeneic graft heart (*day 1*), untransplanted control heart (BALB), untransplanted control heart (B6), and control lymph node (*A*); and allogeneic graft heart (*day 1*), allogeneic graft heart (*day 7*), untransplanted control heart (BALB), untransplanted control heart (B6), and control lymph node (*B*). The *x*-axis distance is proportional to the dissimilarity between groups.

pendent immune response at *day 7*. Differential gene expression in the microarray data was confirmed in repeat murine cardiac transplants by fluorogenic quantitative PCR assay. In the allogeneic transplants, calpactin I, collagen-α1 (Col3A1), and metallothionein-1 fold change mRNA expression increased at *day 1* relative to control heart (Fig. 7*A*). At *day 7* posttransplant, C1qb expression increased 10-fold relative to control. In addition, calpactin I, Col3A1, and apolipoprotein E are upregulated greater than twofold relative to control at *day 1*. The real-time PCR data in Fig. 7*B* shows greater than twofold downregulation in response to transplantation at *day 1* of myoglobin, LDH2B, myosin light chain 2 (Mylpc), ventricular alkali myosin light chain (Mylc), and troponin-I. Also consistent with the microarray data, at *day 7* posttransplant, real-time PCR expression of creatine kinase, cytochrome C oxidase ViaH, decorin, lactate dehydrogenase 2B, myoglobin, myosin light chain 2, smooth muscle γ-actin, troponin-I, and ventricular alkali myosin light chain are all downregulated (Fig. 7). These results all correlate with the temporal increase in Δz relative to control observed in the microarray data. An exception, calpactin I shows a relatively low Δz and a robust fold change at *day 1*. This is likely from a low amount of calpactin I mRNA present in the control heart, whereby any change in mRNA expression at *day 1* will result in a high fold change relative to control heart.

DISCUSSION

It is well established that the infiltration and activation of inflammatory cells is an important component of allograft rejection. Our hypothesis is that graft responses to transplant injury are important in initiating pro-inflammatory stimuli that amplify subsequent immunity. Our results identify subsets of genes and ESTs that are candidates to mediate this graft response.

Changes in expression of genes constitutively expressed in heart, but not lymph node tissue, should be enriched for graft genes responding to transplant injury. However, we cannot exclude that some genes were constitutively expressed only in heart tissue and subsequently upregulated in inflammatory cells following transplantation. Importantly, based on the degree of dissimilarity generated in the dendrogram between the control lymph node and the three graft heart groups, it is likely that most genes remain differentially expressed following transplantation. Also, the selection of heart-restricted subset genes with modulated expression in both the allogeneic group and alymphoid group should identify genes regulated indepen-

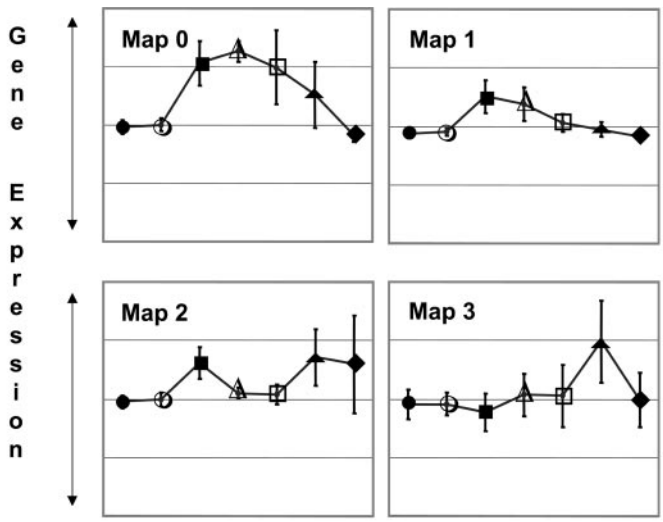

Fig. 6. SOMs of expression following transplantation of genes constitutively expressed in neither heart nor lymph node. Clusters of genes with similar patterns of expression in the experimental groups were identified using SOMs. Experimental groups distributed on *x*-axis include untransplanted BALB control heart (●), untransplanted B6 control heart (○), alymphoid graft heart (*day 1*) (■), allogeneic graft heart (*day 1*) (△), alymphoid graft heart (*day 7*) (□), allogeneic graft heart (*day 7*) (▲), and control lymph node (◆). The *y*-axis is relative gene expression, which is auto-scaled to enhance visualization and thus variable among the profiles. The mean expression is depicted as the symbols with error bars indicating 2 standard deviations. The number of genes in each cluster is 10 (*cluster 0*), 6 (*cluster 1*), 2 (*cluster 2*), and 9 (*cluster 3*). The algorithm was initiated with 2 × 2 geometry using 100 epochs. Genes corresponding to each map are listed in Table 3.

Table 3. *Neither heart- nor lymph node-restricted subset self-organizing map output*

Map	ID	Abbreviation	Description	Gene Ontology Biological Process (secondary biological process)
Map 0	X81627	24p3	24p3	cell growth and/or maintenance (transport)
	V00755	IFN-β	interferon-β	developmental processes (histogenesis and organogensis)
Map 1	V00719	α-amylase	liver α-amylase	metabolism (carbohydrate metabolism)
	X16151	Eta-1	early T-lymphocyte activation 1	cell communication (cell adhesion), developmental processes (ossification),
	M18194	Fibronectin	fibronectin	cell communication (cell adhesion)
	X67644	gly96	gly96	cell growth/maintenance
	W13166	ngal	ma93f11.r1 EST	cell growth and/or maintenance (transport)
	X51834	Osteopontin	osteopontin	cell communication (cell adhesion), developmental processes (ossification)
	L28835	Pxmp2	peroxisome membrane protein	cell growth and/or maintenance (peroxisome organization and biogenesis)
	X91824	SPRR1a	SPRR1a	cell organization/biogenesis (cytoskeleton)
Map 2	AA109527	Actb	ml95g08.r1 EST	cell organization/biogenesis (cytoskeleton organization and biogenesis)
	W41745	Fcer1g	mc63b06.r1 EST	defense response
Map 3	X62742	H2-DMa	Ma	defense response
	W11156	IP-30	clone 316417 similar to IP-30	defense response (immune response)
	U34277	PAF	PAF acetylhydrolase	defense response (inflammatory response) metabolism (membrane lipid metabolism)
	X03479	SAA 3	serum amyloid A3	defense response (acute phase response)

Genes identified in each map output are listed in alphabetical order.

dently of adaptive immunity. *Map 1* of the SOM of heart only subset genes (see Fig. 3 and Table 2) contains six such genes. Among the known genes, metallothionein-1 is induced by stress including exposure to heavy metals. Interestingly, metallothionein has also been shown to provide protection against electrophiles and oxidant stress and to be induced during acute liver injury and regeneration (24). Similarly, αB2-crystallin, a member of the heat shock protein family, is a negative regulator of apoptosis that acts distally in the conserved cell death apparatus by interfering with the maturation of caspase-3 (14). αB2-crystallin is upregulated by ischemia in congestive heart failure (27) and upregulated in an ischemia/reperfusion model in swine (7). Collagen type 3 is produced by myofibroblasts following ischemia in response to angiotensin II, fibroblast growth factor, platelet-derived growth factor, atrial natriuretic factor, prostaglandin E_2, and nitric

Table 4. *Modulated genes allogeneic day 1 posttransplant*

Description	Identifier	Change in *z* at *day 1*	Biological Process
Upregulated genes *day 1*			
αB2-crystallin gene	M73741	4.55	developmental processes
MT-1 metallothionein-1	V00835	2.82	stress response
COL3A1 collagen-α1	X52046	1.30	cell communication
Actg2 smooth muscle γ-actin	U20365	0.85	cell growth/maintenance
Calpactin I heavy chain	D10024	0.83	defense response
Cathepsin D	X52886	0.69	metabolism
Cysteine-rich glycoprotein SPARC	X04017	0.58	cell growth/maintenance
HB-EGF	U39192	0.55	cell growth/maintenance
Heat shock protein (HSP47)	D12907	0.44	cell communication
mSUG1	Z54219	0.37	cell growth/maintenance
Downregulated genes *day 1*			
Cytcox cytochrome c oxidase subunit ViaH	U08439	−1.37	metabolism
LDH2B lactate dehydrogenase 2B	X51905	−1.56	metabolism
PGII (decorin)	X53929	−1.58	metabolism
β-Enolase	X61600	−1.69	metabolism
Myoglobin	X04405	−2.88	metabolism
Mylpc myosin light chain	M91602	−3.41	cell growth/maintenance
Mylc ventricular alkali myosin light chain	X67685	−4.75	cell growth/maintenance
Trop troponin-1	Z22784	−5.21	cell growth/maintenance
α-Cardiac myosin heavy chain	M76601	−5.96	cell growth/maintenance
CK muscle creatine kinase	X03233	−5.98	metabolism

Expression values were normalized and expressed in standard deviation (*z*) units.

Table 5. *Modulated genes allogeneic day 7 posttransplant*

Description	Identifier	Change in z at *day 7*	Biological Process
Upregulated genes *day 7*			
C1q C	X66295	4.809	defense response
Apolipoprotein E	D00466	3.532	cell growth/maintenance
C1qa	X58861	2.780	defense response
C1q B chain	M22531	2.674	defense response
Col3A1 collagen-α1	X52046	2.575	cell communication
MT-1 metallothionein 1	V00835	1.699	stress response
αB2-crystallin	M73741	1.619	developmental processes
Calpactin I heavy chain	D10024	1.574	defense response
C1Q C precursor	ET62967	1.522	defense response
pro-α2(I)collagen	X58251	1.087	cell communication
Downregulated genes *day 7*			
PGII (decorin)	X53929	−2.150	metabolism
β-Enolase	X61600	−2.302	metabolism
Lactate dehydrogenase 2B	X51905	−2.516	metabolism
Cyt-cox cytochrome c oxidase	U08439	−3.073	metabolism
Mylpc myosin light chain	M91602	−6.232	cell growth/maintenance
α-Cardiac myosin heavy chain	M76601	−7.306	cell growth/maintenance
Mylc ventricular alkali myosin light chain	X67685	−7.847	cell growth/maintenance
CK muscle creatine kinase	X03233	−8.936	metabolism
Trop troponin-I	Z22784	−10.179	cell growth/maintenance
Myoglobin	X04405	−12.713	metabolism

oxide (22). Thus previously reported functions of genes in *map 1* genes are consistent with induction due to transplantation injury. *Maps 2* and *3*, which show overlapping profiles of expression, include genes downregulated following transplantation. Members of these maps such as creatine kinase, lactate dehydrogenase, and troponin-I are released following myocardial ischemia. Decorin, a small proteoglycan produced by vascular smooth muscle cells, has been shown to inhibit TGF-β and diminish fibrosis (10).

Analysis of genes constitutively expressed in neither heart nor lymph node, but detected following transplantation in both the alymphoid and allogeneic groups, identified a subset of inducible genes (see Fig. 6 and Table 3). *Map 0*, and to a lesser extent *map 1*, in the SOM identified several pro-inflammatory genes. Members of these maps include interferon-β, a cytokine shown to be important in innate immune responses and in interactions with cells of the adaptive immune system and 24p3, a lipocalin acute phase response protein that has been suggested to function as a regulator of inflammation (15). Eta-1/osteopontin, a cytokine produced by multiple cell types including chondrocytes, has been shown to promote T_H1 T cell responses (2). Gly96 which is highly expressed in fibroblasts, is an immediate early gene with a short half-life inducible by serum growth factors (3), and fibronectin has been shown to modulate TGF-β induction of IL-8 (26). Because all of these genes are upregulated in both the alymphoid and syngeneic groups, the mechanism appears to be independent of adaptive immunity. Interestingly, *maps 2* and *3* contain genes detected during the late phase of rejection (*day 7*) and include the interferon inducible IP-30, the antigen processing gene Ma, and serum amyloid A3 which is a major contributor to the acute phase response. Based on previously reported functions, some of these genes may be induced by the severe injury to the graft including myocyte necrosis that is caused by the rejection process.

The differential expression of graft genes following transplantation illustrates the involvement of the innate immune response. Identification of the genes with the greatest difference in gene expression between normalized control heart and normalized experimental data sets further demonstrates the involvement of stress and innate immunity. Comparison of the genes with the largest positive change relative to control in *days 1* and *7* posttransplantation shows both groups include αB2-crystallin, a negative regulator of apoptosis (14), the cytoprotectant metallothionein-1, collagen-α1, the smooth muscle cell mitogen HBEGF, the lysosomal protease cathepsin D, SPARC, and calpactin I, a binding site related to macrophage migration. Consistent with ischemic injury and eventual graft rejection, genes with the largest negative change at *days 1* and *7* include myoglobin, troponin-I, creatine kinase, and α-cardiac myosin heavy chain. High αB2-crystallin expression at *day 1* is likely in response to the ischemia and reperfusion of transplantation. αB2-crystallin is upregulated in an ischemia reperfusion model in swine (7) and is noted to be a negative regulator of apoptosis that acts distally in the conserved cell death apparatus by interfering with the maturation of caspase-3 (14). At *day 7*, the four graft genes with the largest change in normalized expression values were C1qc, apolipoprotein E, C1qa, and C1qb. C1q is a member of the innate immune system that is involved in pattern recognition and opsonization of foreign particles. C1q initiates the classic complement pathway via binding to IgG or IgM that has bound to antigen. In skin grafting experiments, C4 knockout mice deficient in classic pathway activation have a notably impaired antibody response

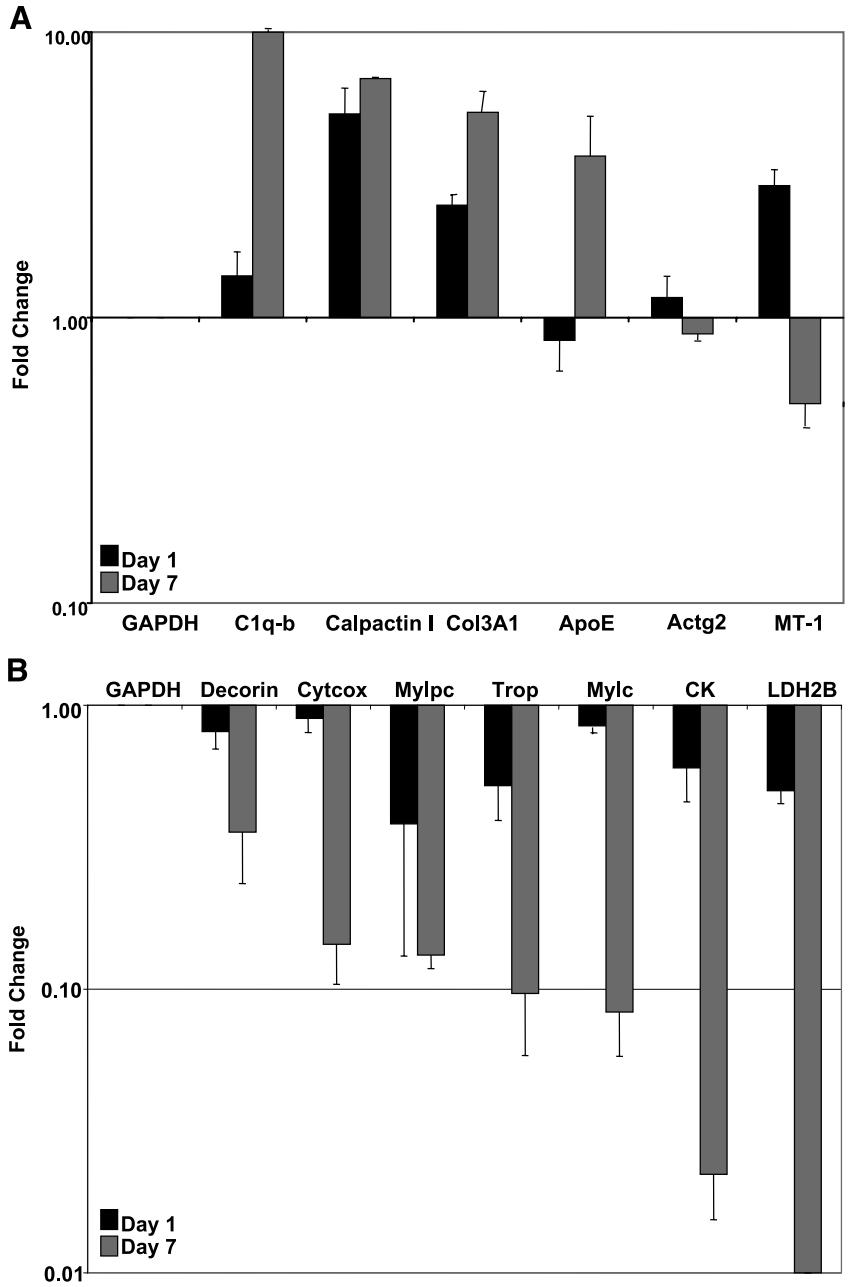

Fig. 7. Independent verification of microarray quantification. *A*: relative mRNA levels of C1qb subunit, calpactin I, collagen-α1 (Col3A1), apolipoprotein E (ApoE), metallothionein-1 (MT-1), smooth muscle γ-actin (Actg2) genes. *B*: relative mRNA levels of decorin, cytochrome C oxidase ViaH (Cytcox), troponin-I (Trop), creatine kinase (CK), lactate dehydrogenase 2B (LDH2B), myosin light chain 2 (Mylpc), and ventricular alkali myosin light chain (Mylc) genes. Relative mRNA levels were measured via the increase in fluorescence caused by the binding of SYBR Green to double-stranded DNA produced during PCR amplification. Real-time PCR data is shown in fold change ($2^{-\Delta CT}$) relative to control heart.

against donor tissue antigens (16). In xenografts, experimental inhibition of the interaction between C1q and immunoglobulin prolongs graft survival (9). Experimental evidence support the role of apolipoprotein E in the modulation of the immune response. Apolipoprotein E antagonizes growth-factor-induced lymphocyte proliferation (17). Compared with normal mice, apolipoprotein E-deficient mice fail to suppress early proliferation of *Listeria monocytogenes* (21) and are more susceptible to *Klebsiella pneumoniae* endotoxemia (6).

Our experimental design used DNA microarrays to investigate gene expression in response to transplantation injury. The advantage of this approach is the feasibility of readily analyzing large numbers of genes, whereas the limitation is the lack of information on protein expression or function of individual genes. Caution must be exercised when evaluating microarray data. With the large numbers of genes analyzed, false positives are likely to occur. Evaluating genes on fold changes can magnify the importance of genes expressed at very low levels with changes that are relatively small compared with genes expressed at higher levels. Also, calculating the change between normalized gene expression data sets may not include genes with low baseline expression and small but significant changes that may be important in the process of rejection. In this analysis, we separately included aspects of both fold change (dendrograms and SOM) and change between normalized data sets (Δz). Our control consti-

tutive expression data were obtained by hybridizing samples onto two GeneChips. Data obtained posttransplantation was hybridized to one GeneChip per experimental condition. Microarray patterns of gene expression in highly differentiated genes were independently verified in repeated transplants in triplicate by real-time PCR. The genes identified in each of our experimental groups using clustering algorithms and SOM are highly consistent with previously reported functions. Thus we believe that these observations do indeed provide a framework to evaluate specific genes and functions in future studies.

A possible limitation to our approach is the inability to distinguish genes expressed by graft tissue and infiltrating cells. We have elected to analyze the graft in total but limited our analysis to genes not expressed in control lymph node. By focusing on genes expressed constitutively in untransplanted heart and following those particular genes posttransplant, we gain insight into the gene modulation of the graft tissue. Genes expressed in the neither subset are a mixture of upregulated graft genes and infiltrating cell genes. Our experimental design does not differentiate inducible gene expression of infiltrating cells from graft cells. Studies in progress will focus on purifying cell populations infiltrating the graft and evaluating differential gene expression of infiltrating cells vs. graft cells during rejection.

Further limiting our gene expression profile study is the inability to measure gene expression in individual graft cell populations such as myocytes, endothelial cells, and fibroblasts during rejection. Cardiac fibroblasts are known to proliferate and synthesize collagen following acute injury and hypoxia-reoxygenation (20). Fibroblasts isolated from rejecting cardiac allografts show increased proliferation in cell culture (12). Although fibroblast activation is more commonly associated with chronic rejection, expression profiles of the fibroblast-enriched myocardial interstitium may be helpful in elucidating peri-transplant cellular responses that precede formation of graft-destructive fibrosis, coronary vasculopathy, and cardiac allograft hypertrophy. In cardiac allograft rejection, myocytes undergo necrosis and apoptosis resulting from cytotoxic T lymphocyte-myocyte interaction. Apoptosis of interstitial and endothelial cells is present in heart allografts and may contribute to the vascular injury associated with allograft rejection. Future studies to elucidate the gene expression profiles from individual cell populations should provide insight into the mechanisms of cardiac myocyte death and vascular injury.

The data presented in our study on the graft response lead us to consider the following hypothesis: Local production of the innate immune collectin C1q subspecies (C1qa, C1qb, C1qc) are important for acute rejection via apoptotic cell clearance. C1q, a member of the classic complement cascade, has the ability to bind C-reactive protein and serum amyloid P component and activate the classic complement pathway (18). Additionally, C1q has been shown to bind to and stimulate ingestion of apoptotic cells in vitro (19) and to enhance apoptotic cell uptake in vivo (25). Further understanding of the role of C1q and apoptosis and transplant rejection may illuminate the mechanisms involved in cardiac myocyte, endothelial, and interstitial cell death and may give clues into therapeutic targets aimed at suppressing allograft rejection.

Current therapeutic strategies to prevent allograft rejection are designed to inhibit the adaptive immune response, in particular, T cell responses. Our analysis of changes in gene expression attributed to the graft tissue in response to transplantation injury provides insights into the graft response to transplantation prior to and during T cell activation.

DISCLOSURES

This work was supported by an American Heart Association Established Investigator Award, an Arthritis Foundation Research Award, and National Institutes of Health Grant RO1-AI-44085 (all to D. L. Perkins).

REFERENCES

1. **Ashburner M, Ball CA, Blake JA, Botstein D, Butler H, Cherry JM, Davis AP, Dolinski K, Dwight SS, Eppig JT, Harris MA, Hill DP, Issel-Tarver L, Kasarskis A, Lewis S, Matese JC, Richardson JE, Ringwald M, Rubin GM, and Sherlock G.** Gene ontology: tool for the unification of biology. The Gene Ontology Consortium. *Nat Genet* 25: 25–29, 2000.
2. **Ashkar S, Weber GF, Panoutsakopoulou V, Sanchirico ME, Jansson M, Zawaideh S, Rittling SR, Denhardt DT, Glimcher MJ, and Cantor H.** Eta-1 (osteopontin): an early component of type-1 (cell-mediated) immunity. *Science* 287: 860–864, 2000.
3. **Charles CH, Abler AS, and Lau LF.** cDNA sequence of a growth factor-inducible immediate early gene and characterization of its encoded protein. *Oncogene* 7: 187–190, 1992.
4. **Christopher K, Mueller TF, Ma C, Liang Y, and Perkins DL.** Analysis of the innate and adaptive phases of allograft rejection by cluster analysis of transcriptional profiles. *J Immunol* 169: 522–530, 2002.
5. **Corry RJ, Winn HJ, and Russell PS.** Heart transplantation in congenic strains of mice. *Transplant Proc* 5: 733–735, 1973.
6. **de Bont N, Netea MG, Demacker PN, Verschueren I, Kullberg BJ, van Dijk KW, van der Meer JW, and Stalenhoef AF.** Apolipoprotein E knock-out mice are highly susceptible to endotoxemia and *Klebsiella pneumoniae* infection. *J Lipid Res* 40: 680–685, 1999.
7. **Depre C, Tomlinson JE, Kudej RK, Gaussin V, Thompson E, Kim SJ, Vatner DE, Topper JN, and Vatner SF.** Gene program for cardiac cell survival induced by transient ischemia in conscious pigs. *Proc Natl Acad Sci USA* 98: 9336–9341, 2001.
8. **Eisen MB, Spellman PT, Brown PO, and Botstein D.** Cluster analysis and display of genome-wide expression patterns. *Proc Natl Acad Sci USA* 95: 14863–14868, 1998.
9. **Fryer JP, Leventhal JR, Pao W, Stadler C, Jones M, Walsh T, Zhong R, Zhang Z, Wang H, Goodman DJ, Kurek M, d'Apice AJ, Blondin B, Ivancic D, Buckingham F, Kaufman D, Abecassis M, Stuart F, and Anderson BE.** Synthetic peptides which inhibit the interaction between C1q and immunoglobulin and prolong xenograft survival. *Transplantation* 70: 828–836, 2000.
10. **Fukui N, Fukuda A, Kojima K, Nakajima K, Oda H, and Nakamura K.** Suppression of fibrous adhesion by proteoglycan decorin. *J Orthop Res* 19: 456–462, 2001.
11. **He H, Stone JR, and Perkins DL.** Analysis of robust innate immune response after transplantation in the absence of adaptive immunity. *Transplantation* 73: 853–861, 2002.

12. **Hellkvist J, Tufveson G, Gerdin B, and Johnsson C.** Characterization of fibroblasts from rejecting tissue: the hyaluronan production is increased. *Transplantation* 74: 1672–1677, 2002.
13. **Ideker T, Thorsson V, Ranish JA, Christmas R, Buhler J, Eng JK, Bumgarner R, Goodlett DR, Aebersold R, and Hood L.** Integrated genomic and proteomic analyses of a systematically perturbed metabolic network. *Science* 292: 929–934, 2001.
14. **Kamradt MC, Chen F, and Cryns VL.** The small heat shock protein αB-crystallin negatively regulates cytochrome c- and caspase-8-dependent activation of caspase-3 by inhibiting its autoproteolytic maturation. *J Biol Chem* 276: 16059–16063, 2001.
15. **Liu Q and Nilsen-Hamilton M.** Identification of a new acute phase protein. *J Biol Chem* 270: 22565–22570, 1995.
16. **Marsh JE, Farmer CK, Jurcevic S, Wang Y, Carroll MC, and Sacks SH.** The allogeneic T and B cell response is strongly dependent on complement components C3 and C4. *Transplantation* 72: 1310–1318, 2001.
17. **Mistry MJ, Clay MA, Kelly ME, Steiner MA, and Harmony JA.** Apolipoprotein E restricts interleukin-dependent T lymphocyte proliferation at the G1A/G1B boundary. *Cell Immunol* 160: 14–23, 1995.
18. **Nauta AJ, Bottazzi B, Mantovani A, Salvatori G, Kishore U, Schwaeble WJ, Gingras AR, Tzima S, Vivanco F, Egido J, Tijsma O, Hack EC, Daha MR, and Roos A.** Biochemical and functional characterization of the interaction between pentraxin 3 and C1q. *Eur J Immunol* 33: 465–473, 2003.
19. **Ogden CA, deCathelineau A, Hoffmann PR, Bratton D, Ghebrehiwet B, Fadok VA, and Henson PM.** C1q and mannose binding lectin engagement of cell surface calreticulin and CD91 initiates macropinocytosis and uptake of apoptotic cells. *J Exp Med* 194: 781–795, 2001.
20. **Piacentini L and Karliner JS.** Altered gene expression during hypoxia and reoxygenation of the heart. *Pharmacol Ther* 83: 21–37, 1999.
21. **Roselaar SE and Daugherty A.** Apolipoprotein E-deficient mice have impaired innate immune responses to *Listeria monocytogenes* in vivo. *J Lipid Res* 39: 1740–1743, 1998.
22. **Sutton MG and Sharpe N.** Left ventricular remodeling after myocardial infarction: pathophysiology and therapy. *Circulation* 101: 2981–2988, 2000.
23. **Tamayo P, Slonim D, Mesirov J, Zhu Q, Kitareewan S, Dmitrovsky E, Lander ES, and Golub TR.** Interpreting patterns of gene expression with self-organizing maps: methods and application to hematopoietic differentiation. *Proc Natl Acad Sci USA* 96: 2907–2912, 1999.
24. **Theocharis SE, Kanelli H, Margeli AP, Spiliopoulou CA, and Koutselinis AS.** Metallothionein and heat shock protein expression during acute liver injury and regeneration in rats. *Clin Chem Lab Med* 38: 1137–1140, 2000.
25. **Vandivier RW, Ogden CA, Fadok VA, Hoffmann PR, Brown KK, Botto M, Walport MJ, Fisher JH, Henson PM, and Greene KE.** Role of surfactant proteins A, D, and C1q in the clearance of apoptotic cells in vivo and in vitro: calreticulin and CD91 as a common collectin receptor complex. *J Immunol* 169: 3978–3986, 2002.
26. **Wang AC and Fu L.** Fibronectin regulates the activation of THP-1 cells by TGF-β1. *Inflamm Res* 50: 142–148, 2001.
27. **Yang J, Moravec CS, Sussman MA, DiPaola NR, Fu D, Hawthorn L, Mitchell CA, Young JB, Francis GS, McCarthy PM, and Bond M.** Decreased SLIM1 expression and increased gelsolin expression in failing human hearts measured by high-density oligonucleotide arrays. *Circulation* 102: 3046–3052, 2000.